Nuclear Materials and Energy 000 (2016) 1–6

Contents lists available at ScienceDirect

Nuclear Materials and Energy

journal homepage: www.elsevier.com/locate/nme

# TEM analysis of recrystallized double forged tungsten after exposure in JUDITH 1 and JUDITH 2

W. Van Renterghem[a,*], I. Uytdenhouwen[a], Th. Loewenhoff[b], M. Wirtz[b]

[a] SCK • CEN, The Belgian Nuclear Research Centre, Boeretang 200, 2400 Mol, Belgium
[b] Forschungszentrum Jülich GmbH, Institut für Energie- und Klimaforschung - Werkstoffstruktur und -eigenschaften, 52425 Jülich, Germany

ARTICLE INFO

*Article history:*
Received 13 November 2015
Revised 24 March 2016
Accepted 5 April 2016
Available online xxx

*Keywords:*
Tungsten
Edge localized mode
Transmission electron microscopy

ABSTRACT

Five samples of recrystallized pure tungsten were exposed to transient heat loads using the electron beam of the JUDITH 1 and JUDITH 2 installations of Forschungszentrum Jülich. The heat flux and base temperature were the same for all samples; only the number of pulses and exposure device differed. Transmission electron microscopy was applied to determine the first defects that are introduced during exposure and to compare the effects of the two machines. With increasing number of pulses, first dislocations are formed near the grain boundaries, and then line dislocations and clusters of dislocations appear within the grains. Upon prolonged exposure, the dislocations migrate and cluster in dislocation pile-ups. Comparing exposure in JUDITH 1 to JUDITH 2, the amount of defects is much higher in the samples exposed in JUDITH 1.



## 1. Introduction

Tungsten is the main candidate material to be used in the divertor and as a first wall material in future fusion reactors. During operation, the integrity of the first wall material will be affected by the interaction with the plasma. The most frequently occurring interactions are the so-called edge localized modes (ELMs), during which a high amount of energy is periodically loaded on the plasma facing materials in a very short time [1,2]. This results in a local heating at the surface of the plasma facing material, which generates thermal stresses. Depending on the heat load, pulse time, number of pulses and base temperature, ELMs can induce a broad range of effects from surface roughening up to crack formation and local melting [3].

Furthermore, the defect structure in the sub-surface area is changed by the thermal stresses. In a previous experiment [4], a recrystallized tungsten sample, which did not contain defects apart from large angle grain boundaries, was exposed to high heat loads. The defect structure after exposure was found to consist of a large number of small angle grain boundaries. In the experiments presented in this paper a much lower heat load was applied and the conditions were selected to induce no visible damage. The aim of the study is to verify if these low heat loads will also introduce defects in the material and, if so, how these defects can explain the formation of small angle grain boundaries that were observed at higher heat loads.

A second aim of the study is to compare the effects of an exposure in the JUDITH 1 machine to the JUDITH 2 machine. In previous studies [5], only double forged but not re-crystallized tungsten was exposed in JUDITH 2. The TEM results on these samples could hardly identify a change in defect structure because the material before exposure already contained a large amount of defects and small grain boundaries in particular. Repeating these exposures on recrystallized tungsten allows determining the effect of exposure in JUDITH 2 on the sub-surface defect structure.

## 2. Experimental

The tungsten material was produced by Plansee AG applying cold isostatic pressing of homogenized powder, followed by sintering at 2000–2500 °C and forging into a rod. A second forging step in the axial direction was applied, with the intention to create a homogenous material, but resulting in disc shaped grains. At last the disk was annealed at 1000 °C for stress relieving. Five samples were cut, with dimensions of 12 mm × 12 mm × 5 mm. After grinding and polishing, all samples were recrystallized by a heat treatment at 1600 °C for 1 h to be sure that no deformation from

* Corresponding author.
*E-mail addresses:* wvrenter@sckcen.be (W. Van Renterghem), iuytdenh@sckcen.be (I. Uytdenhouwen), T.Loewenhoff@fz-juelich.de (Th. Loewenhoff), M.Wirtz@fz-juelich.de (M. Wirtz).

http://dx.doi.org/10.1016/j.nme.2016.04.003

**Table 1**
Sample exposure conditions in JUDITH 1 and 2 (heat flux factor, number of pulses and base temperature).

| Name | Heat flux factor $F_{HF}$ ($MW/m^2s^{1/2}$) | Number of pulses | Base temperature $T_{base}$ (°C) | Machine |
|---|---|---|---|---|
| V5 | 3 | 1E+02 | 200 | JUDITH 1 |
| V6 | 3 | 1E+03 | 200 | JUDITH 1 |
| W8 | 3 | 1E+03 | 150–200 | JUDITH 2 |
| W7 | 3 | 1E+04 | 150–200 | JUDITH 2 |
| W6 | 3 | 1E+05 | 150–200 | JUDITH 2 |

the material production or the final preparation before exposure remains [4].

The exposures were performed in Forschungszentrum Jülich in the JUDITH 1 and JUDITH 2 installations. The exposure conditions are summarized in Table 1. Samples V5 and V6 were exposed in JUDITH 1 during which they were heated to 200 °C by an ohmic heater and loaded with 100, respectively 1000 pulses of 1 ms with a power density of 95 $MW/m^2$ (heat flux factor $F_{HF} = 3\ MW/m^2s^{1/2}$). During each pulse an area of 8 mm by 8 mm is exposed to a fast scanning electron beam with an energy of 120 keV. To avoid heat accumulation by the electron beam, the pulse frequency was $< 0.5$ Hz.

Samples W6, W7 and W8 were brazed to a copper heat sink and exposed in JUDITH 2 (geometry shown in [6]). They were loaded with transients of 0.48 ms duration and power density of 137 $MW/m^2$, resulting in the same heat flux factor as in JUDITH 1 ($F_{HF} = 3\ MW/m^2s^{1/2}$), but with a frequency of 25 Hz to achieve high pulse numbers in reasonable time. The use of hot (100 °C) cooling water and the accumulation of heat due to the high frequency lead to a base temperature of 150–200 °C, which is a close match with the base temperature applied in the JUDITH 1 experiments. The energy of the electrons was 40 keV.

It should be noted that the exposure conditions of samples V6 and W8 were comparable and the results on these two samples will reflect the effect of the exposure machines on the exposure damage.

The effect of the electron beam exposure on the surface of the samples was studied with a scanning electron microscope (SEM) on a JEOL 6610LV instrument before further sample preparation for the TEM investigation.

The sample preparation for TEM analysis aimed at obtaining samples as close to the exposed surface as possible. The procedure described in [4], including single side grinding and single jet electro-polishing, was applied. To study the reference material, two platelets were taken from the non-exposed edges of samples V5 and W7. On these platelets both sides were grinded and the area that was analyzed, laid at least 300 μm below the surface.

The specimens were investigated with TEM on a JEOL 3010 microscope operating at 300 kV.

## 3. Results

### 3.1. Reference

To clearly determine the effect of the electron exposure, the reference material obtained from the exposed samples was studied as well. Fig. 1a shows a typical bright field image of the reference material taken from sample V5. No defects can be observed in the interior of the grains. The grain boundaries are large angle grain boundaries as proven by the diffraction pattern in Fig. 1b. In this diffraction pattern, reflections are observed generated in all three grains of Fig. 1a. Even though the exact orientation was not determined, it is clear that the orientation differs more than a few degrees. This defect structure is typical for recrystallized tungsten. At several locations along the grain boundaries, small dislocation-like contrast can be observed which interferes with the fringe contrast induced by the grain boundaries.

For comparison, a similar image of the defect structure of the reference material taken from sample W7 is shown in Fig. 1c. This image confirms that the only defects are large-angle grain boundaries. Contrary to the reference sample of sample V5, no defects disrupting the fringe contrast induced by the grain boundary were found here.

### 3.2. Sample V5 (100 pulses, JUDITH 1)

In Fig. 2a, a SEM image of the exposed loaded surface can be found. No surface modification such as roughening, plastic deformation or crack formation was seen.

The exposure to the electron beam JUDITH 1 induced the creation of defects in the recrystallized tungsten, but the distribution is not homogeneous. Several locations were found where still no defects were present. At other locations a limited number of line dislocations were formed. They were identified as a/2 <111> type screw dislocations, the typical dislocations in tungsten materials.

Whereas the majority of the observed dislocations were isolated line dislocations, clusters of tangled line dislocations were found at some locations. One example of such a cluster is shown in Fig. 2b. A high density of dislocations was formed in an area of less than 1 μm by 1 μm. The presence of these clusters indicates that the

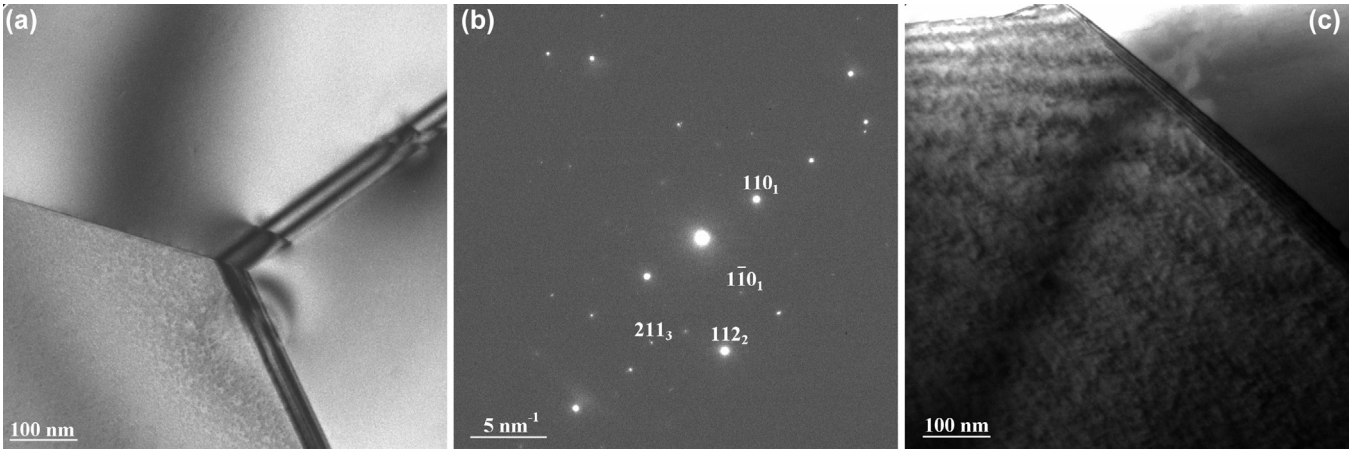


**Fig. 1.** (a) bright field image of the defect structure in the reference material obtained from sample V5. (b) The corresponding diffraction pattern. (c) Bright field image of a grain boundary in sample W7.

Please cite this article as: W. Van Renterghem et al., TEM analysis of recrystallized double forged tungsten after exposure in JUDITH 1 and JUDITH 2, Nuclear Materials and Energy (2016), http://dx.doi.org/10.1016/j.nme.2016.04.003

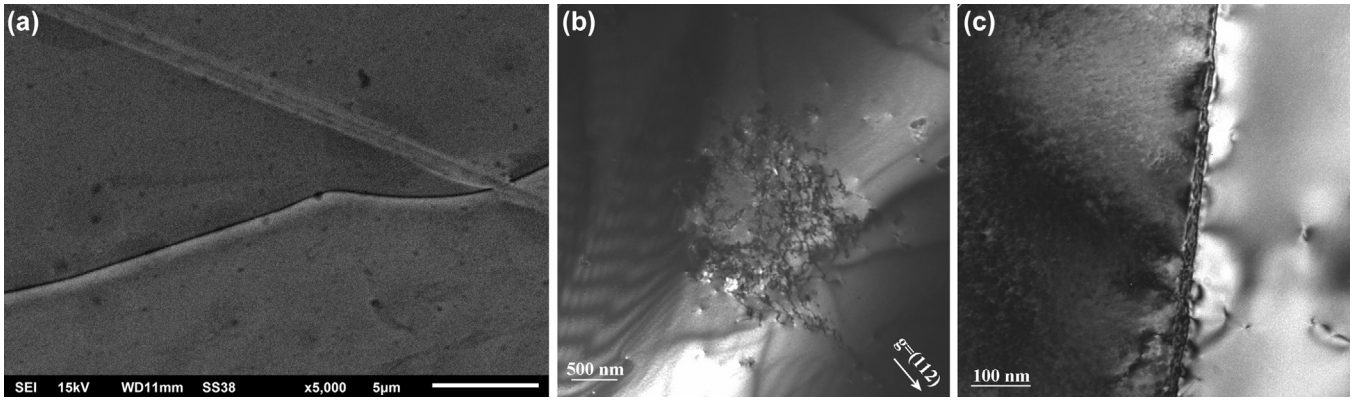


**Fig. 2.** (a) SEM image of sample V5 in the middle of the exposed area. No roughening or crack formation could be found. (b) Dark field image of a cluster of dislocations close to the exposed surface. (c) Bright field image at a grain boundary.

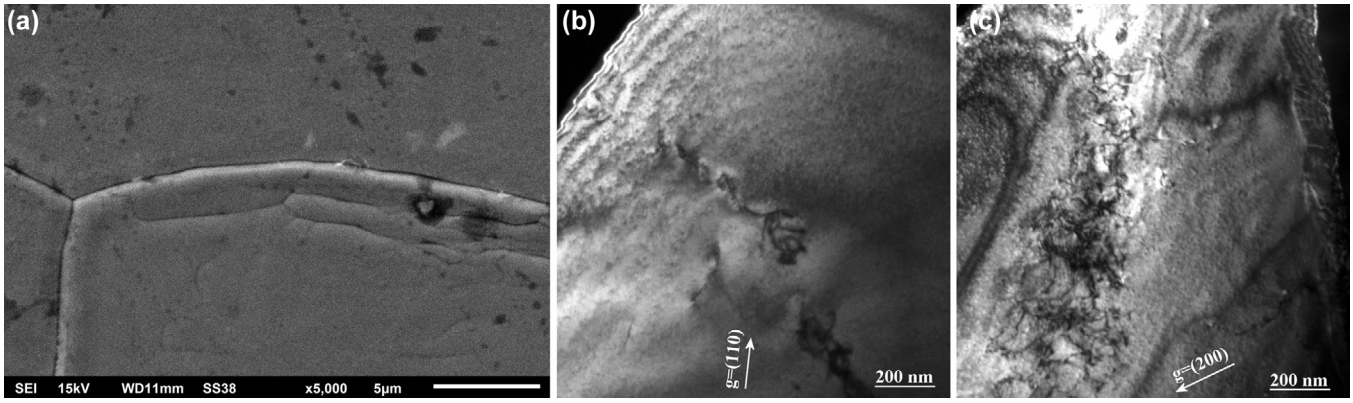


**Fig. 3.** (a) SEM image of the heat loaded surface area of sample V6, revealing the formation of dislocation pile-ups close to the grain boundaries. (b) Dark field image of small dislocation clusters. (c) Dark field image of a pile-up of tangled line dislocations close to a large-angle grain boundary (right side of the image).

electron beam exposure induces high local stresses, which result in the formation of a high number of dislocations. The tangling pins these dislocations and prevents their movement to form a homogeneous distribution.

Fig. 1c shows the defect structure at a high angle grain boundary. In the reference material from the same sample, it was observed that stress induced defects were formed at the boundary. In the part of the sample closer to the exposed surface, it was found again that defects are occurring at the grain boundary and that they induce stress fields. The number of such defects has increased compared to the reference.

### 3.3. Sample V6 (1000 pulses, JUDITH 1)

The SEM images in Fig. 3 still did not show any changes in the surface morphology such as roughening, plastic deformation or crack formations. However, in the area close to the grain boundaries, some features were observed, which indicate local defect formation and which are probably resulting from large dislocation pile-ups.

The TEM investigation of sample V6 revealed that the amount of defects increased significantly. Contrary to sample V5, no areas that are free of defects were found anymore. Moreover, the amount of line dislocations has increased. Fig. 3b shows an area with a limited number of dislocations. Some line dislocations are still isolated, but in general the dislocations are tangled forming small dislocation clusters.

At other locations, preferentially located near a grain boundary, pile-ups of tangled dislocations were observed, see Fig. 3c. In a previous study on recrystallized tungsten exposed at higher temperature and to higher heat loads, it was found that the small angle grain boundaries that were removed during the recrystallization heat treatment, were formed again [4]. In sample V6, the dislocation pile-up does not form a small-angle grain boundary yet, but it can be expected that these pile-ups of dislocations result in small-angle grain boundaries after exposing under more severe loading conditions.

In the right part of Fig. 3c, a grain boundary can be observed. Apart from the grain boundary fringe contrast, several line dislocations can be observed. It confirms the suggestion from the reference material that defects are preferentially formed at the grain boundaries.

### 3.4. Sample W8 (1000 pulses, JUDITH 2)

Sample W8 was exposed under similar conditions as sample V6, but the exposure was performed in the JUDITH 2 machine. Therefore, the comparison of the defect structures in these two samples will reveal the effect of the exposure device. Fig. 4 shows the general defect structure in sample W8. No large clusters of dislocations or dislocation pile-ups were found. The only defects that were found in this sample were a limited number of line dislocations. In Fig. 4a four dislocations can be observed which seem to be aligned, while in Fig. 4b the dislocations are tangled. In both cases it is obvious that the amount of defects introduced during exposure in JUDITH 2 is much lower than in JUDITH 1, at least in the area about 10 μm below the exposure surface.

Please cite this article as: W. Van Renterghem et al., TEM analysis of recrystallized double forged tungsten after exposure in JUDITH 1 and JUDITH 2, Nuclear Materials and Energy (2016), http://dx.doi.org/10.1016/j.nme.2016.04.003

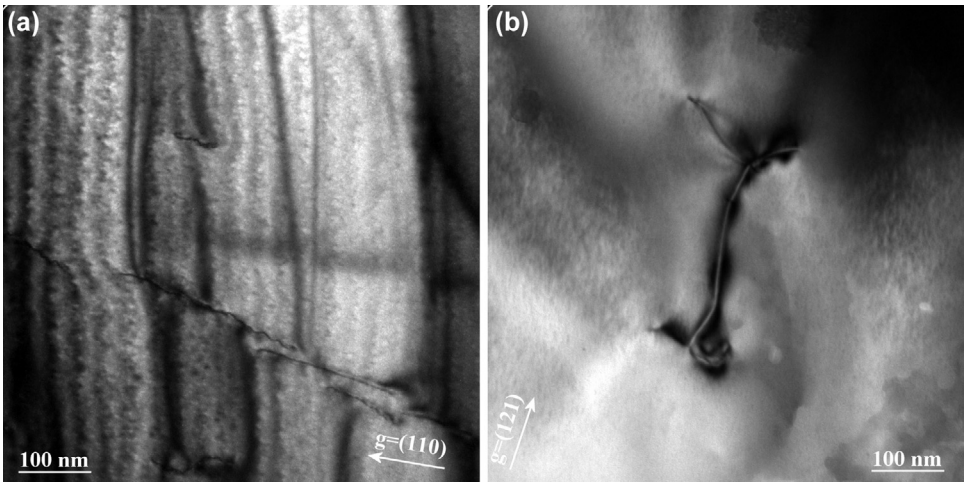


**Fig. 4.** (a) Bright field image of a few individual, but aligned dislocations in sample W8. (b) Bright field image of a small number of tangled dislocations.

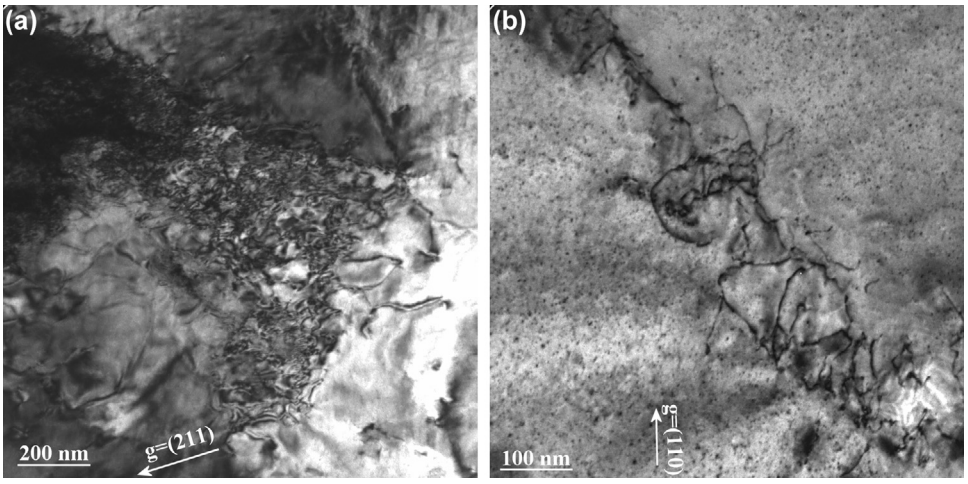


**Fig. 5.** (a) Bright field image of a cluster of dislocations in sample W7 and (b) bright field image of a dislocation pile-up.

### *3.5. Sample W7 ($10^4$ pulses, JUDITH 2)*

Fig. 5a and b shows bright field images obtained from the single jet polished sample. Areas were found that were free of defects, but at other locations in the same sample, defects were formed as a result of the exposure. Fig. 5a shows an example of a cluster consisting of a large number of tangled dislocations and Fig. 5b shows a series of tangled dislocations forming a dislocation pile-up. The trend that more defects are formed with an increasing number of pulses also applies for the JUDITH 2 exposures, even though the total number of dislocations is much lower than after exposure in JUDITH 1.

### *3.6. Sample W6 ($10^5$ pulses, JUDITH 2)*

The general defect structure is shown in Fig. 6. Fig. 6a focuses on one of the large-angle grain boundaries. The areas in the grain adjacent to the boundaries are free of defects. However, the fringe contrast of the boundary itself, shows some additional contrast which can be attributed to line dislocations.

Other areas of the grain interior are not free of defects. Fig. 6b shows an example of a site where several line dislocations are tangled into a small cluster. Compared to the other JUDITH 2 samples, there are more dislocations than in sample W7 or W8, but the large dislocation clusters or dislocation pile-ups like in sample V5 and V6 were not found.

## 4. Discussion

### *4.1. Effect of number of pulses*

The conditions of the electron beam exposures were selected as such that the topography of the surface would hardly be affected. The base temperature is set to 150–200 °C, while the low heat flux factor of 3 $MW/m^2\ s^{1/2}$ will only induce an additional maximum temperature rise of ~170 °C. It should be noted that this low heat flux factor gives a power density of less than 0.2 $GW/m^2$, which was reported as the damage threshold [3]. The heat load and number of pulses are too low to create detrimental surface effects. No evidence of cracking or severe surface roughening was found in the SEM analyses of the samples.

The TEM investigation of the defect structure revealed that even these mild exposure conditions, which did not result in macroscopic damage, changed the microstructure. The material was selected to contain no defects, apart from large-angle grain boundaries, before the exposure. Hereto double forged tungsten was subjected to a recrystallization treatment after the cutting, grinding and polishing to remove defects introduced during manufacture and the mechanical preparation. It was proven that this heat treatment removes all defects from the tungsten [4] and the successful application was confirmed in two reference samples.

Because no defects were present in the reference material, all defects that were found in the TEM images are induced by the

Please cite this article as: W. Van Renterghem et al., TEM analysis of recrystallized double forged tungsten after exposure in JUDITH 1 and JUDITH 2, Nuclear Materials and Energy (2016), http://dx.doi.org/10.1016/j.nme.2016.04.003

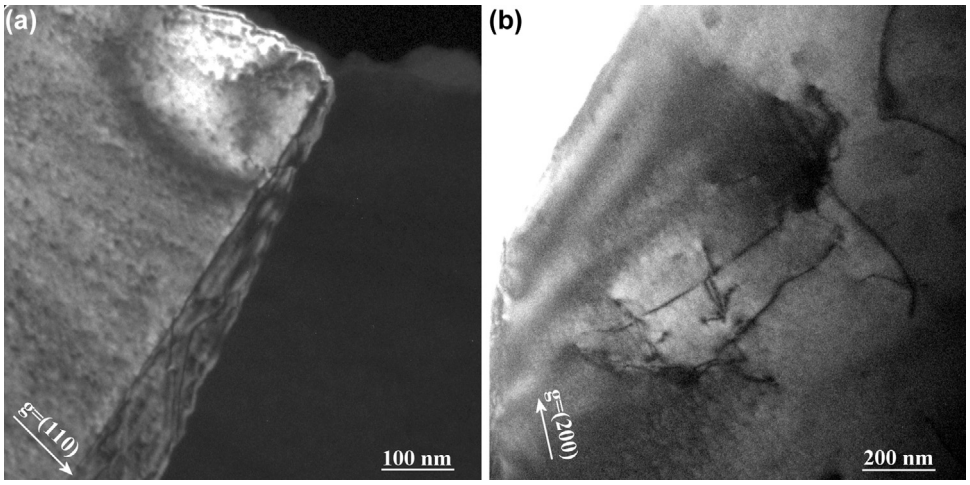


**Fig. 6.** (a) Dark field image of a grain boundary in sample W6. The fringe contrast of the boundary is affected by line dislocations. (b) Bright field image of a cluster of line dislocations.

electron beam exposure. The local temperature increase induces thermal stresses close to the exposed surface, which are sufficiently high to create defects. Previous examinations on samples exposed to much higher energies, have shown the creation of small-angle grain boundaries [4]. The lower heat loads applied here did not have such a drastic effect. However, some signs of the onset of small-angle grain boundary formation by large dislocation pile-ups were seen by SEM images in the highest pulse number sample of JUDITH 1. The main defects that were found were line dislocations. The overall concentration of dislocations was still low and often large areas that were free of defects were found. As a general trend, the number of dislocations increased with an increasing number of pulses. The observed defect structure is indicative of the early stages of thermal fatigue, which may lead to macroscopic damage at increased number of pulses.

The distribution of dislocations is very inhomogeneous. At various locations in the samples, clusters of tangled dislocations or dislocation pile-ups were found. More defects were found in the samples exposed in JUDITH 1 and it seems that in the samples exposed in JUDITH 2, the clusters of dislocations are formed closer to the exposed surface. The very dense clusters of dislocations that were found locally indicate that the stress introduced by the heat load is very high and local. With increasing number of pulses, more and more dislocation pile-ups are being formed. The continued stress enforcement will induce dislocation movement, and results in dislocation pile-up formation. In the present exposure, the pile-ups in the TEM images do not mark a difference in grain orientation, but it is believed that these dislocation pile-ups are the onset of the formation of the small angle grain boundaries at more severe exposure conditions.

Based on these observations, a sequence of defect evolution can be proposed. The defects at the grain boundaries will be formed first. This is evidenced by the fact that they occur in all exposed samples and even in a sample further away from the surface where no other defects were found. The next step is the formation of individual line dislocations. With increasing number of pulses, fewer defect free areas and more small clusters of tangled dislocations were present. Moreover, dense clusters are formed indicating high local stress. The repeated stress during the exposure pulses causes the dislocations to move until they become immobile in a dislocation tangle or agglomerate into dislocation pile-ups. The final step, which was not observed in the samples analyzed in this study, is the conversion of these dislocation pile-ups into small-angle grain boundaries.

Even though no macroscopic damage was observed at the surface, the TEM investigation revealed permanent changes of the defect structure. With increasing number of pulses, the number of created dislocations increases as well. This indicates the beginning of a fatigue damage, which may eventually result in surface damage at even higher number of pulses. This fatigue damage was already observed experimentally in low power density high pulse number tests [7]. The formation of cracks due to single or few strong thermal shocks is already understood to a certain extent and was also simulated successfully by different groups [8,9]. However, fatigue damage which becomes relevant for PFM provided the thermal shocks are mitigated to avoid immediate damage is much more complex and demands a deeper understanding of microscopic processes. This study proofs that an accumulation or evolution with increasing number of thermal shock pulses exists and gives an insight in the first stages of this development.

### 4.2. Comparison JUDITH 1 and JUDITH 2

One of the aims of this TEM analysis is to compare the effect of the device on the exposure induced defect structure, while applying the same exposure parameters. There are a number of differences in operation between the two installations. The first difference is the energy of the electrons. For JUDITH 1 the electrons are accelerated to 120 kV, while in JUDITH 2 the accelerating voltage is only 40 kV. The higher energy electrons will penetrate deeper into the material and they will deposit their energy further down the surface. Monte Carlo simulations have shown that the penetration depth for tungsten increases from 5 μm to 7 μm when increasing the acceleration voltage from 40 to 120 kV. This is a rather small difference and simulations as well as experiments [10,11] have shown no difference in damage formation compared to laser exposure (near zero penetration), at least for macroscopic damage.

A second difference is the global stress state due to fixing and preheating of the samples. For JUDITH 1 the entire sample is heated by an ohmic heater to $T_{base}=200\,°C$ and fixed in a copper holder with screws. The pulse frequency is ~0.5 Hz to avoid heat accumulation and allow the surface to cool down to the $T_{base}$ before each pulse. The heating in JUDITH 2, on the other hand, is partly achieved by using hot cooling water (100 °C, similar to the ohmic heater a homogeneous temperature throughout the sample) and partly by the heat accumulation due to the frequency of the pulses of 25 Hz which is necessary to achieve high number of pulses. This results in a small temperature gradient (50–100 °C)

Please cite this article as: W. Van Renterghem et al., TEM analysis of recrystallized double forged tungsten after exposure in JUDITH 1 and JUDITH 2, Nuclear Materials and Energy (2016), http://dx.doi.org/10.1016/j.nme.2016.04.003

from the top surface to the cooling tube wall (about 8 mm deeper). The samples are brazed to the copper heat sink and are thus restricted at the bottom.

Electron beam loading (beam guidance) itself is also different in the machines: JUDITH 1 uses a scanning technique using two high frequency deflection systems for the *x*- and *y*-direction. The thin (FWHM ~1 mm) but intense beam scans a 4 × 4 mm² area with 40–50 kHz for 1 ms. This results in a loading that is inhomogeneous in time ("spiky"), however the envelope is a rectangle. JUDITH 2 has a broader beam (FWHM ~12 mm) which is used as described in [12] being nearly stationary during the transient pulse (max. power density variation 10%). This results in a truly rectangular load in time with slight wobbles. Loading in JUDITH 2 is thus more homogeneous in time.

The differences in exposure methods have a large effect on the resulting defect structure. In the samples that were prepared a few micrometers below the surface, the JUDITH 1 exposure introduces significantly more dislocations in that area, which resulted in dislocation clusters and pile-ups. In the samples exposed in JUDITH 2 fewer defects were observed even though the number of pulses was equal or higher than in the samples exposed in JUDITH 1. As an explanation for this difference, it appears that the more homogeneous exposure conditions in JUDITH 2 result in smaller thermal stresses, which limits the driving force for dislocation formation. Further verification of this statement is planned on samples exposed with laser irradiation, which would be even more homogeneous than the JUDITH 2 exposure.

## 5. Conclusions

Five samples of recrystallized double forged pure tungsten were exposed to the electron beam of the JUDITH 1 and JUDITH 2 installations of Forschungszentrum Jülich. The heat flux and base load were the same for all samples, only the number of pulses and exposure device differed. The exposure conditions were selected to induce no cracking or surface roughening. The aim of the investigation is to determine the first defects that are introduced during exposure and to compare the effects of the two machines.

The reference materials were found to contain no defects apart from large-angle grain boundaries, which means that all observed defects are introduced during the exposure. The main defects are a/2⟨111⟩ screw type line dislocations. The dislocations appeared as individual dislocations, dense clusters of tangled dislocations and dislocation pile-ups. It was shown that exposure conditions that do not introduce any macroscopic damage still lead to permanent changes of the microstructure.

With increasing number of pulses the amount of defect-free areas decrease and the number of dislocations increased, which indicates a fatigue damage process. First dislocations are formed near the grain boundaries. Then line dislocations and clusters are formed. Upon prolonged exposure, the dislocations migrate and cluster in dislocations pile-ups. These dislocation pile-ups are the onset of the formation of small angle grain boundaries observed in previous experiments. These basic mechanisms in W lead to macroscopic surface damage in the long run.

There is a large difference in defect structure formed in JUDITH 1 compared to JUDITH 2, where the amount of defects is much higher in the samples exposed in JUDITH 1. The exposure conditions in JUDITH 2 are more homogeneous and it is proposed that this leads to lower local stress which would explain the observation. Future experiments with a laser are planned to further investigate this point.

## Acknowledgment

This work has been carried out within the framework of the EUROfusion Consortium and has received funding from the Euratom research and training programme 2014-2018 under grant agreement No. 633,053. The views and opinions expressed herein do not necessarily reflect those of the European Commission.

## References

[1] A. Loarte, M. Becoulet, G. Saibene, R. Sartori, D.J. Campbell, et al., Plasma Phys. Control. Fusion 44 (2002) 1815–1844.
[2] R.A. Pitts, S. Carpentier, F. Escourbiac, T. Hirai, V. Komarov, et al., J. Nucl. Mater. 438 (2013) S48–S56, doi:10.1016/j.jnucmat.2013.01.008.
[3] G. Pintsuk, A. Prokhodtseva, I. Uytdenhouwen, J. Nucl. Mater. 417 (2011) 481, doi:10.1016/j.jnucmat.2010.12.109.
[4] W. Van Renterghem, I. Uytdenhouwen, Fus. Eng. Des. 88 (2013) 1650, doi:10.1016/j.fusengdes.2013.05.011.
[5] W. Van Renterghem, I. Uytdenhouwen and Th. Loewenhoff, Proceedings of the 14th International Conference on "Plasma Facing Materials & Components for Fusion Applications" Jülich , Germany, May 13–17 (2013), Poster A044.
[6] Th. Loewenhoff, Combined steady state and high cycle transient heat load simulation with the electron beam facility JUDITH 2, PhD thesis. RWTH Aachen, 2012, http://publications.rwth-aachen.de/record/197556.
[7] Th. Loewenhoff, J. Linke, G. Pintsuk, C. Thomser, Fus. Eng. Des. 87 (2012) 1201–1205, doi:10.1016/j.fusengdes.2012.02.106.
[8] M. Li, E. Werner, J.-H. You, Nucl. Mater. Energy 2 (2015) 1–11, doi:10.1016/j.nme.2014.10.001.
[9] A. Arakcheev, D.I. Skovorodin, A.V. Burdakov, A.A. Shoshin, S.V. Polosatkin, et al., J. Nucl. Mater 467 (2015) 165–171 Part 1, doi:10.1016/j.jnucmat.2015.09.034.
[10] M. Wirtz, Thermal shock behaviour of different tungsten grades under varying preconditions, PhD thesis. RWTH Aachen, 2012, http://publications.rwth-aachen.de/record/62897
[11] M. Wirtz, J. Linke, G. Pintsuk, L. Singheiser, M. Zlobinski, J. Nucl. Mater 438 (2013) S833–S836, doi:10.1016/j.jnucmat.2013.01.180.
[12] Th. Loewenhoff, T. Hirai, S. Keusemann, J. Linke, G. Pintsuk, A. Schmidt, J. Nucl. Mater 415 (2011) S51–S54, doi:10.1016/j.jnucmat.2010.08.065.